

Chapter 3

Pair transfer in a nutshell

3.1 Simultaneous versus successive Cooper pair transfer in nuclei

Cooper pair transfer is commonly thought to be tantamount to simultaneous transfer. In this process a nucleon goes over through the NN -interaction v , the second one does it making use of the correlations with its partner (cf. Figs. 3.1.1 and 5.C.1 (I)). Consequently, in the independent particle limit, simultaneous transfer should not be possible (see Sect. 5.C.1). Nonetheless, it remains operative. This is because, in this limit, the particle transferred through v does it together with a second one which profits from the non-orthogonality of the wavefunctions describing the single-particle motion in target and projectile (Figs. 3.1.2 and 5.C.1 (II)). This is the reason why this (non-orthogonality) transfer amplitude has to be treated on equal footing with the previous one representing, within the overcomplete basis employed, a natural contribution to simultaneous transfer (cf. also the discussion carried out in Ch.2 in connection with the overlap Ω_n Eq. (2.1.3)). In other words, $T^{(1)}$ gives the wrong cross section, even at the level of simultaneous transfer, as it violates two-nucleon transfer sum rules¹. In fact $(T^{(1)} - T_{NO}^{(1)})$ is the correct, sum rule conserving two-nucleon transfer amplitude to lowest order (first) in v (Fig. 3.1.2). The resulting cancellation is quite conspicuous in actual nuclei, in keeping with the fact that Cooper pairs are weakly correlated systems (see e.g. Figs. 3.4.2 (b) and 3.4.3, see also Fig. 3.4.4). This is the reason why the successive transfer process in which v acts twice (implying the mean field U in the post-post representation²), is the dominant mechanism in pair transfer reactions (within this context see Sect. 3.3). While this mechanism seems antithetical to the transfer of correlated fermions pairs (bosons), it probes, in the nuclear case, the same pairing correlations as simultaneous transfer does (Sect. 3.4). This is because nuclear Cooper pairs (quasi-bosons) are quite extended objects, the two nucleons being

¹ Broglia, R. A. et al. (1972), Bayman, B. F. and Clement (1972); cf. also Chapter 1 Sect. 1, 2
² Potel, G. et al. (2013a), Eq. (A7).

see

166

CHAPTER 3. SIMULTANEOUS VERSUS SUCCESSIVE TRANSFER



(virtually) correlated over distances much larger than typical nuclear dimensions⁽³⁾ (cf. Fig. 3.1.3) cf. also Sect. 2.6.1). In a two-nucleon transfer process this virtual property becomes real, in the sense that the presence of (normal) density over regions larger than that of the dimensions of each of the interacting nuclei allows for incipient ξ nuclear Cooper pair manifestation, the difference between the character of simultaneity and of succession becoming strongly blurred.

Within this context, let us refer to the Josephson effect, associated with the Cooper pair tunneling across a thin barrier separating two metallic superconductors. Because the probability of one-electron-tunneling is of the order of 10^{-10} , (conventional) simultaneous tunneling associated with a probability of $(10^{-10})^2$ would hardly be observed (cf. Sect 3.3). Nonetheless, Josephson currents are standard measures in low temperature laboratories⁽⁴⁾.

The same arguments related to the large value of the correlation length is operative in explaining the fact that Coulomb repulsion is rather weak between partners of Cooper pairs which are, in average, at a distance $\xi (\approx 10^4 \text{ \AA})$ much larger than the Wigner-Seitz radius r_s typical of metallic elements ($\approx 1 - 2 \text{ \AA}$). Consequently, it can be overwhelmed by the long range electron phonon pairing. Similarly, in widely extended light halo nuclei, the short range bare pairing interaction plays little role, becoming subcritical (cf. Sect. 2.6). The fact that such systems are nonetheless bound, although weakly, testifies to the dominant role the exchange of collective vibrations between halo nucleons have in binding the associated halo Cooper pair (e.g. $^{11}\text{Li}(\text{gs})$, and, arguably, also⁽⁵⁾ of $^{12}\text{Be} (0^{++}; 2.251 \text{ MeV})$ to the core $^9\text{Li}(\text{gs})$ and ^{10}Be respectively) (cf. Section 6.1.2 and Fig. 6.1.4).

The above arguments are at the basis of the fact that second order DWBA theory which add both successive and non-orthogonality contributions to the simultaneous transfer amplitudes, provides a quantitative account of the experimental findings (see e.g. Figs. 2.2.1, 3.4.2 (a), 3.4.3 (a) and Chapter 6).

3.2 Two-nucleon transfer probabilities, enhancement factor

As discussed in Chapter 1 the enhancement factor in a two-nucleon transfer reaction can be defined in terms of two-particle units⁽⁶⁾, similar to what is done in the case of electromagnetic decay (Weisskopf units⁽⁷⁾). Let us, for simplicity, write such

⁽⁶⁾ Within this context one can put the following question. Is anybody worried that a photon can, in a two slit experiment, be broken in two? No. Why should then one worry that successive transfer can break a Cooper pair?

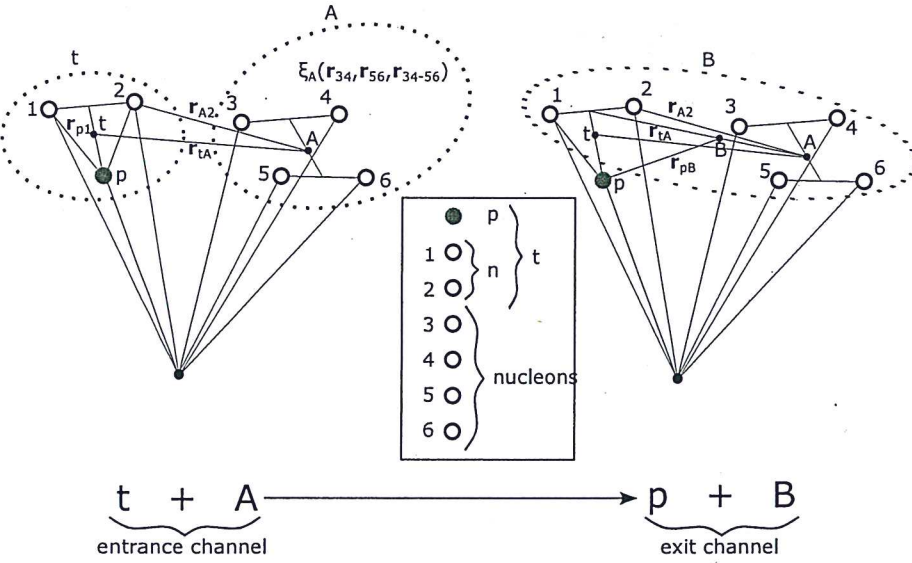
⁽⁷⁾ Cf. e.g. Rogalla and Kes (2012) and references therein.

⁽⁸⁾ See e.g. Johansen et al. (2013).

⁽⁹⁾ Cf. e.g. Broglia, R. A. et al. (1972); Broglia, R.A. et al. (1973) and references therein.

⁽¹⁰⁾ See e.g. Bohr and Mottelson (1969).

↙ draw better



$$\frac{d\sigma}{d\Omega} = \frac{\mu_i \mu_f}{(2\pi\hbar^2)^2} \frac{k_f}{k_i} |T^{(1)} + T_{succ}^{(2)} - T_{NO}^{(1)}|^2$$

$$\phi_t(\mathbf{r}_{p1}, \sigma_1, \mathbf{r}_{p2}, \sigma_2) \chi_{m_s}^{1/2}(\sigma_p) \psi_A(\xi_A) \chi_{tA}^{(+)}(\mathbf{r}_{tA}) \quad \chi_{m_s}^{1/2}(\sigma_p) \psi_B(\xi_B) \chi_{pB}^{(-)}(\mathbf{r}_{pB}).$$

$$(\phi_d(\mathbf{r}_{p1}, \sigma_1) \phi_d(\mathbf{r}_{p2}, \sigma_2) \chi_{tA}^{(+)}(\mathbf{r}_{tA}))$$

$$\Psi_{A+2}(\xi_A, \mathbf{r}_{A1}, \sigma_1, \mathbf{r}_{A2}, \sigma_2) = \psi_A(\xi_A) \sum_{l_i, j_i} [\phi_{l_i, j_i}^{A+2}(\mathbf{r}_{A1}, \sigma_1, \mathbf{r}_{A2}, \sigma_2)]_0^0$$

$$= \psi_A(\xi_A) \sum_{nm} a_{nm} [\varphi_{n, l_i, j_i}^{A+2}(\mathbf{r}_{A1}, \sigma_1) \varphi_{m, l_i, j_i}^{A+2}(\mathbf{r}_{A2}, \sigma_2)]_0^0$$

$$T^{(1)} = 2 \sum_{\sigma_1, \sigma_2, \sigma_p} \int d\xi_A d\mathbf{r}_{tA} d\mathbf{r}_{p1} d\mathbf{r}_{p2} \psi_A(\xi_A) \sum_{l_i, j_i} [\phi_{l_i, j_i}^{A+2}(\mathbf{r}_{A1}, \sigma_1, \mathbf{r}_{A2}, \sigma_2)]_0^0$$

$$\times \chi_{pB}^{(-)*}(\mathbf{r}_{pB}) \chi_{m_s}^{1/2*}(\sigma_p) v(r_{p1}) \phi_t(\mathbf{r}_{p1}, \sigma_1, \mathbf{r}_{p2}, \sigma_2) \chi_{m_s}^{1/2}(\sigma_p) \psi_A(\xi_A) \chi_{tA}^{(+)}(\mathbf{r}_{tA})$$

$$= 2 \sum_{\sigma_1, \sigma_2, \sigma_p} \int d\mathbf{r}_{tA} d\mathbf{r}_{p1} d\mathbf{r}_{A2} \sum_{l_i, j_i} [\phi_{l_i, j_i}^{A+2}(\mathbf{r}_{A1}, \sigma_1, \mathbf{r}_{A2}, \sigma_2)]_0^0$$

$$\times \chi_{pB}^{(-)*}(\mathbf{r}_{pB}) \chi_{m_s}^{1/2*}(\sigma_p) v(r_{p1}) \phi_t(\mathbf{r}_{p1}, \sigma_1, \mathbf{r}_{p2}, \sigma_2) \chi_{m_s}^{1/2}(\sigma_p) \chi_{tA}^{(+)}(\mathbf{r}_{tA})$$

It is of

✓ Figure 3.1.1: Contribution of simultaneous transfer, in first order DWBA, to the reaction $A(t, p)B (\equiv A + 2)$. The nucleus A is schematically assumed to contain four nucleons, the triton being composed of two neutrons and one proton. The set of coordinates used to describe the entrance and exit channels are shown in the upper part, while in the lower part the simultaneous two-nucleon transfer amplitude is written in detail (cf. Potel, G. et al. (2013b)). Of notice that the expression of $T^{(1)}$ violates, in the independent particle basis used, the two-nucleon transfer sum rule by exactly $T_{NO}^{(1)}$, amplitude operative also in lowest order of v (Fig. 3.1.2; see also text). It is of notice that of all the relative motion coordinates, only those describing the relative motion of (t, A) and of (p, B) have asymptotic values.

λ

App. 5 C

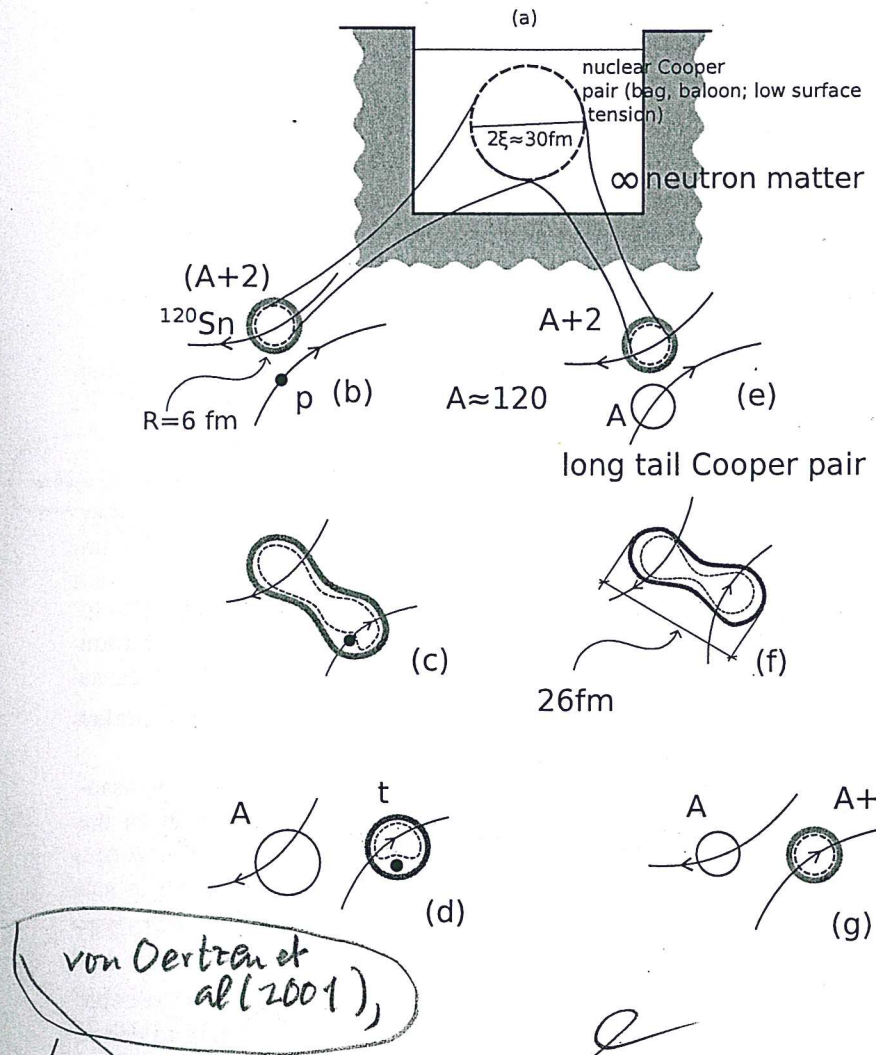


Figure 3.1.3: The correlation length associated with a nuclear Cooper pair is of the order of $\xi \approx \hbar v_F / \Delta \approx 30$ fm (see App. 3.4). (a) in neutron matter at typical densities of the order of 0.5–0.8 saturation density, the $NN^{-1}S_0$ short range force, eventually renormalized by medium polarization effects, makes pairs of nucleons moving in time reversal states to correlate over distances of the order of 5–6 times typical nuclear radii. How can one get evidence for such an extended object? Certainly not when the Cooper bag (balloon) is introduced in (b) the mean field of a superfluid nucleus which, acting as an external field, constrains the Cooper pair to be within the nuclear radius with some spill out (long tail of Cooper pair, grey, shaded area extending outside the nuclear surface defined by $R_0 = 1.2A^{1/3}$ fm). But yes in (c), (d), that is, in the case of two-nucleon transfer process (e.g. (p, t) reaction) in which the absolute cross section can change by orders of magnitude in going from pure two-particle (uncorrelated configurations) to long tail Cooper pair spill outs. This effect is expected to become stronger by allowing pair transfer between similar superfluid nuclei, in which case one profits of the same type of correlations (superfluidity) as resulting from very similar pair mean fields (e), (f), (g) (cf. e.g. von Oertzen, W. (2013) and references therein; see also Eqs. (2.1.2) and (2.1.3)). For the case under discussion $\Omega_n = 1$). Within this context, it is apparent that pairs of nucleons will feel equally well pairing correlations whether they are transferred simultaneously or one after the other (cf. (c) and (f)).

larger than nuclear dimensions
Handly
likely
situations like
close parenthesis

where

$$f(\theta) = \frac{1}{k} \sum_l (2l+1) e^{i\delta_l} \sin \delta_l P_l(\cos \theta), \quad (3.2.6)$$

δ_l being the partial wave l phase shift. Let us now use for simplicity the results associated with hard sphere scattering⁹ in the low and high energy limit. Making use of the fact that in the case under discussion the phase shifts δ_l are related to the regular and irregular spherical Bessel functions,

$$\tan \delta_l = \frac{j_l(kR)}{n_l(kR)}, \quad (3.2.7)$$

and that $\sin^2 \delta_l = \tan^2 \delta_l / (1 + \tan^2 \delta_l)$, one can write in the case in which $kR \ll 1$, i.e. in the low-energy, long wavelength, regime

essentially

$$\tan \delta_l \approx \frac{-(kR)^{2l+1}}{(2l+1)[(2l-1)!!]^2}, \quad (3.2.8)$$

implying that one can ignore all δ_l with $l \neq 0$. Because $\delta_0 = -kR$ (cf. (3.2.7)) regardless the value of k , one obtains,

$$\frac{d\sigma}{d\Omega} = \frac{\sin^2 \delta_0}{k^2} = R^2, \quad (3.2.9)$$

and thus

$$\sigma_{tot} = \int \frac{d\sigma}{d\Omega} d\Omega = 4\pi R^2 \quad (kR \ll 1), \quad (3.2.10)$$

a cross section which is four times the geometric cross section πR^2 , namely the area of the disc of radius R that blocks the propagation of the incoming (plane) wave, and has the same value as that of a hard sphere. Because $kR \ll 1$ implies long wavelength scattering, it is not surprising that quantal effects are important, so as to overwhelm the classical picture. Let us now consider the high energy limit $kR \gg 1$. The total cross section is in this case, given by

$$\begin{aligned} \sigma_{tot} &= \int |f_l(\theta)|^2 d\Omega = \frac{1}{k^2} \int_0^{2\pi} d\phi \int_{-1}^1 d(\cos \theta) \sum_{l=1}^{kR} \sum_{l'=1}^{kR} (2l+1)(2l'+1) \\ &\times e^{i\delta_l} \sin \delta_l e^{-i\delta_{l'}} \sin \delta_{l'} P_l P_{l'} = \frac{4\pi}{k^2} \sum_{l=1}^{kR} (2l+1) \sin^2 \delta_l = \frac{4\pi}{k^2} \sum_{l=1}^{kR} (2l+1) p_l. \end{aligned} \quad (3.2.11)$$

Making use of the relation

$$\sin^2 \delta_l = \frac{\tan^2 \delta_l}{1 + \tan^2 \delta_l} = \frac{[j_l(kR)]^2}{[j_l(kR)]^2 + [n_l(kR)]^2} \approx \sin^2 \left(kR - \frac{\pi l}{2} \right), \quad (3.2.12)$$

⁹f. e.g. Sakurai (1994)

compared with the value $R \approx 6$ fm of the radius of ^{120}Sn . Consequently, we are in a situation of type (3.2.15), that is,

$$\sigma_{tot} = 2\pi(6 + 0.5)^2 \text{ fm}^2 \approx 2.7 \text{ b.} \quad \text{see e.g. (3.2.17)}$$

Because typical values of the absolute one-particle cross section associated with the (p, d) reaction mentioned above are few mb (cf. Fig. 4.2.3 right panel) one can use, for order of estimate purposes,

$$P_1 \approx \frac{5.35 \text{ mb}}{2.7 \text{ b}} \approx 10^{-3}, \quad (3.2.18)$$

bring back

as the typical probability for such processes. Consequently, one may argue that the probability for a pair of nucleons to simultaneously tunnel in e.g. the (p, t) process mentioned above is $(P_1)^2 \approx 10^{-6}$, as near impossible as no matter. Within this context we note that the integrated $\text{gs} \rightarrow \text{gs}$ absolute cross section $\sigma(^{120}\text{Sn}(p, t)^{118}\text{Sn(gs)}) \approx 2.5 \pm 0.2$ mb (cf. Figs. 2.2.1 and 6.2.1). This fact implies that the empirical two-nucleon transfer probability is of the order of $P_2 \approx 10^{-3}$. Consequently, $P_2/(P_1)^2 \approx 10^3$, a ratio which can hardly be explained in terms of a physical enhancement factor.

The above contradictions¹² are, to a large extent, connected with the fact that one is addressing the subject of pairing correlations in nuclei as probed by two-nucleon transfer reactions, treating separately the associated questions of structure and reactions, while they are but complementary aspects of the same physics. Let us elaborate on this point.

When one turns on, in an open shell atomic nucleus like e.g. $^{120}_{50}\text{Sn}_{70}$, a pairing interaction of strength larger than critical, the system moves into an independent pair regime¹³ (cf. e.g. Sects. 2.4.1 and 2.4.2 as well as Fig. 2.4.3; see Fig. 3.2.1). This fact has essentially no consequence concerning the one-particle transfer mechanism, exception made regarding the size of the mismatch between the relative motion-incoming ($p + ^{120}\text{Sn(gs)}$) and -outgoing ($d + ^{119}\text{Sn(gs)}$) trajectories (Q -value and recoil effect), in keeping with the fact that one has to break a Cooper pair to populate a single quasiparticle state. From a structure point of view the depletion of the occupation probability measured in a (p, d) process is correlated with the corresponding increase in occupation observed in (d, p) (U^2, V^2 factors). Aside from the quantitative values, this is also observed in dressed single-particle

¹² Within this context it is of notice that similar questions were raised by Bardeen (1962, 1961); Pippard (2012); Cohen et al. (1962); McDonald (2001) in connection with the prediction of Josephson (Josephson (1962)) that there should be a contribution to the current through an insulating barrier between two superconductors which would behave like direct tunneling of condensed pairs. This is in keeping with the fact that a single electron has a probability of $\approx 10^{-10}$ of getting through, the "classical" estimate of simultaneous pair tunneling being $\approx 10^{-20}$, an impossible observation as stated above (cf. App. 3.8).

¹³ Regime which is conditioned by the "external" mean field. In other words, regime which express itself provided there is nucleon density available (see Sect. 3.2). It is of notice that pairing in turn may help extend the range over which nucleon density is available, as in the case of the neutron halo nucleus ^{11}Li .

(normal)

(abnormal density)

$$P_2 = \lim_{\epsilon \rightarrow 0} \left| \frac{1}{\sqrt{2}} (e^{i\phi} U \sqrt{P_1} + e^{i\phi} V \sqrt{P_1}) \right|^2$$

$$= P_1 \lim_{\epsilon \rightarrow 0} \frac{(1 + 2UV \cos \epsilon)}{2} \approx P_1 \quad (\epsilon = \phi - \phi')$$

174 CHAPTER 3. SIMULTANEOUS VERSUS SUCCESSIVE TRANSFER

states, the single-particle sum rule implying both the (A-1) and (A+1) system (see App. 4.I). Concerning the phase coherence of the pair correlated wavefunction it has no consequence for one-particle transfer process, in keeping with the fact that $|e^{i\phi} \sqrt{P_1}|^2 = P_1$.

The situation is very different concerning (Cooper) pair transfer. From a reaction point of view, and in keeping with the non-orthogonality existing between the wavefunctions in target and projectile, the associated contributions to the transfer process have to be eliminated. This is in keeping with the fact that simultaneous two-nucleon transfer can take place also in first order in the proton-neutron interaction v_{np} . When this is a consequence of the correlation between the partners of the Cooper pair (cf. Fig. 5.C.1 (I)) it constitutes a *bona fide* contribution. Not when it is a consequence of non-orthogonality (see Fig. 5.C.1 (II)). Continuing within the realm of reaction theory, second order processes in v_{np} are to be included (Fig. 5.C.2) and as a rule neglect higher orders in keeping with the small value of P_2 ($\approx 10^{-3}$, cf. also Table 6.B.1). Let us now bring structure into the discussion. The fact that the wave function of the nucleons in the pair are phase-coherent ($(U_\nu + V_\nu e^{-2i\phi} a_\nu^\dagger a_\bar{\nu}^\dagger) |0\rangle$) implies that one has to add the amplitudes before one takes modulus squared (cf. also Sect. 3.6 and Sect. 3.7), that is,

$$P_2 = \lim_{\epsilon \rightarrow 0} \left| \frac{1}{\sqrt{2}} (e^{i\phi} \sqrt{P_1} + e^{i\phi} \sqrt{P_1}) \right|^2 = P_1$$

$$= P_1 \lim_{\epsilon \rightarrow 0} \frac{(1 + 2UV \cos \epsilon)}{2} \approx P_1, \quad = P_1 \lim_{\epsilon \rightarrow 0} (1 + \cos \epsilon) = 2P_1 \quad (\epsilon = \phi - \phi'), \quad (3.2.19)$$

again, an unexpected quantum mechanical result as e.g. (3.2.13). Because the range of v_{np} ($a \approx 1$ fm) is much smaller than the correlation length ($\xi \approx 20-30$ fm), in the successive process (3.2.19), the Cooper pair tunnels between target and projectile equally formed and "unharmed" as in the simultaneous process. Think again that in the nuclear pairing correlated system only Cooper pairs exist (in which the partners nucleons are correlated over 20-30 fm from each other) and not single nucleons (normal system) at ≈ 4 fm (2 fm being the radius of the Wigner-Seitz nucleus cell) from each other (Fig. 3.2.1). To the extent that the mean field acting as an "external" field allows particle density to be present, the properties of independent Cooper pair motion will explicit themselves. And thus is a physical condition which is assumed fulfilled each time one will make use of Fig. 3.2.1 (b). In other words, inside ^{120}Sn all Cooper pairs will be found within a volume of radius $R_0 \approx 6$ fm, in the same way in which a Cooper pair will be distributed over two similar volumes during the contact time in e.g. a Sn+Sn heavy ion reaction.

¹⁴ The interest of the picture shown in Fig. 3.2.1 (b) can also be exemplified by referring to a single stable nucleus lying along the stability valley, with the fact that the moment of inertia of heavy deformed nuclei is considerably smaller than the rigid moment of inertia, but still larger than the irrotational one ($5J_{irrot} \lesssim J \lesssim J_{r}/2$). Even confined within the mean field of the nucleus, the small but finite number of pairs of correlated nucleons having the "intrinsic", infinite-matter-like tendency displayed if Fig. 3.2.1 (b), will, to some extent, average out the different orientations of the rotating system and react to it in terms of an effective deformation smaller than the one related to the $B(E2)$

where the assumption is made that $UV \approx 1/2$.

(see also Sect. 3.2). This explains the importance of long-range induced pairing interaction (exchange of phonons) in general, let alone in very extended light halo nuclei like ^{11}Li .

Within this context we note that the (approximate) form of the (local) pair wavefunction can be written as (cf. Leggett (2006) p. 185; for the non local nuclear version cf. e.g. Broglia and Winther (1983))

$$F(r) \approx \Delta N(0) \frac{\sin k_F r}{k_F} \exp\left(\frac{\sqrt{2}r}{\xi}\right), \quad (3.2.20)$$

where $N(0)$ is the density of levels at the Fermi energy for one spin orientation. For $r \leq \xi$ the pair wavefunction is approximately proportional to that of two particles at the Fermi energy moving freely in a relative s -wave state. In a typical metallic superconductor ξ is of the order of 10^4 Å, much larger than the inter electron spacing (≈ 1 Å). Note that relative to the Fermi energy, the correlation energy ($E_{corr} = (-1/2)N(0)\Delta^2$) associated with Cooper pairing is very small, $\approx 10^{-7} - 10^{-8}$. Arguably, the most important consequence of this fact, is the exponentially large radius and thus very small value of the relative momentum associated with Cooper pairs. In other words, the typical scenario for a very small value of the localization kinetic energy and thus of the generalized quantity parameter (cf. App. 6.H), implying that the two partners, are rigidly anchored to each other (Cooper pair). This phenomenon is at the basis of the emergence of new elementary modes of excitation (pairing vibrations for single Cooper pairs, pairing rotations for few ones, supercurrents and Josephson currents for macroscopic amounts of them).

of very extended Cooper pairs

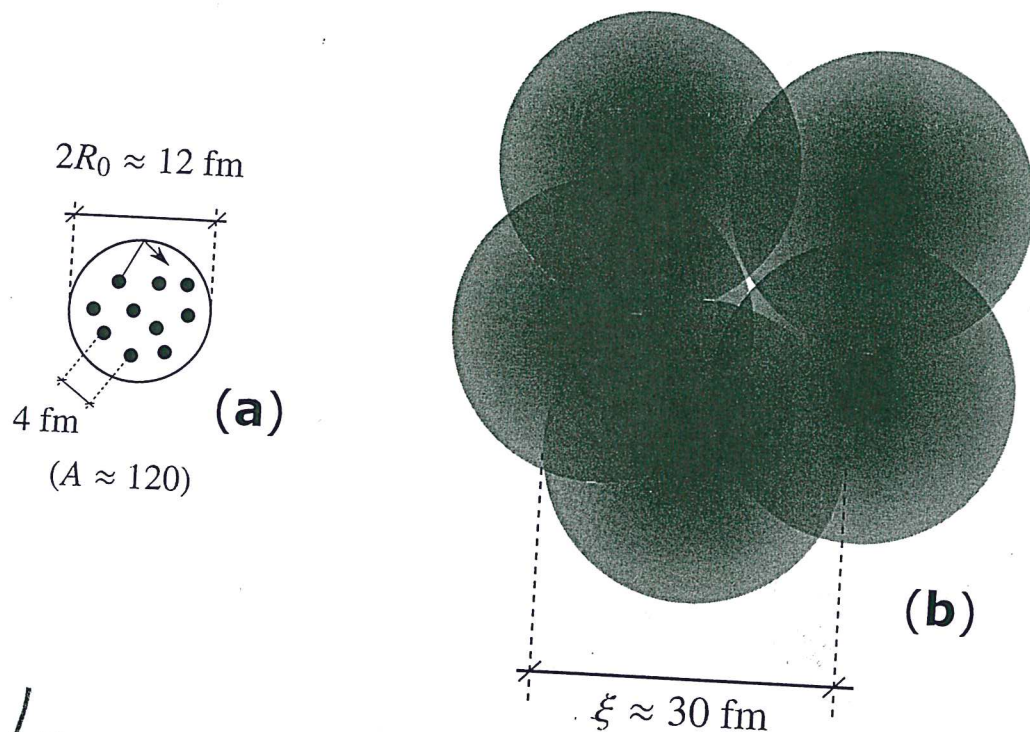
The situation sounds, in principle, very different from atomic nuclei, in keeping with the fact that nuclear Cooper pairs are, as a rule, subject to an overwhelming external (mean) field ($|E_{corr}| \approx 1$ MeV $\ll |U(r \approx R_0)| \approx |V_0/2| \approx 25$ MeV). But even in this case, one can posit that the transition from independent particle to independent pair motion implies that Cooper pair partners recede from each other. Let us clarify this point for the case of a single pair, e.g. $^{208}\text{Pb(gs)}$. It is true that allowing the pair of neutrons to correlate in the valence orbitals leads to a pair wavefunction which is angle correlated ($\Omega_{12} \approx 0$), as compared to the pure $j^2(0)(j = g_{9/2})$ configuration¹⁵. On the other hand, the correlated pair addition mode (Tables 2.5.4 and 2.5.5) will display a sizeable spill out as compared to the pure two particle state, and thus a lower density and larger related average distance between Cooper pair partners. This is also the reason why close to $\approx 40\%$ of the pairing matrix elements is contributed by the induced pairing interaction resulting from the exchange of long wavelength, low-lying, collective modes, the other $\approx 60\%$ resulting from the bare nucleon-nucleon 1S_0 pairing interaction (cf. Fig. 2.6.1). In carrying out the above arguments the values of $(E_{corr}/\epsilon_F)^2 \approx \left(\frac{1 \text{ MeV}}{37 \text{ MeV}}\right)^2 \approx$

in the case of
condensed
matter (e.g.,
low-temperature
superconductors)
than in

collective (rotational) values. However, constrained as they are they cannot fully profit of pairing superfluidity.

¹⁵Bertsch, G. F. et al. (1967), Ferreira, L. et al. (1984); Matsuo, M. (2013).





✓ Figure 3.2.1: (a) Schematic representation of independent-particle motion and (b) independent-pair motion. In the first case nucleons (fermions) move independently of each other reflecting elastically from the wall of the mean field created by all the other nucleons, each of which is associated with a Wigner-Seitz cell of radius $d = ((4\pi/3)R_0^3/A)^{1/3}$ implying a relative distance of $2d$ (the actual numbers correspond to e.g. ^{120}Sn). Switching on the pairing interaction (bare plus induced) leads to Cooper pair formation in which the correlation length is ξ . Thus, pair of nucleons moving in time reversal states close to the Fermi energy will tend to recede from each other lowering their relative momentum ($2d \rightarrow \xi$) thus boosting the stability of the system, provided that the external mean field allows it. Or better, if there is nucleon density available to do so, something controlled to a large extent by the single-particle potential. From this point on, and at least for the levels lying close to the Fermi surface, one cannot talk about particles but about Cooper pairs (unless one does not intervene the system with an external field, e.g. (p, d) and provides the energy, angular and linear momentum needed to break a pair). Of course that the system to the right under the influence of an external field (like e.g. the HF of ^{120}Sn) Cooper pairs will be constrained within its boundaries. But this will be true with two nuclei of ^{120}Sn at a relative (CM) distance much larger than $2R_0$ ($\approx 12 \text{ fm}$). The pair field associated with a Cooper pair will extend from one to the other partner of the heavy ion reaction through the weakly overlapping interaction region, allowing two nucleons to correlate over ξ and, eventually, in a reaction like e.g. $\text{Sn} + \text{Sn} \rightarrow \text{Sn(gs)} + \text{Sn(gs)}$ allow for the transfer of two nucleons correlated over tens of fm.

the picture displayed in (b) will be close to be representative

sensible

10^{-3} and $\xi = \frac{\hbar v_F}{2E_{corr}} \approx 30 \text{ fm} ((\frac{v_F}{c}) \approx 0.3)$, valid for nuclei along the stability valley, were used.

The situation described above becomes clearer, even if extreme, in the case of ^{11}Li . In this case, the Fermi momentum is $k_F \approx 0.8 \text{ fm}^{-1}$, the radius $R \approx 4.58 \text{ fm}$, much larger than $R_0 = 2.7 \text{ fm}$ expected from systematics. Furthermore essentially all of the correlation energy ($E_{corr} \approx 0.5 \text{ MeV}$, $(E_{corr}/\epsilon_F)^2 \approx (0.5/14)^2 \approx 10^{-3}$, $\xi \approx 20 \text{ fm}$ ($v_F/c \approx 0.1$)) is associated with the exchange of the dipole pigmy resonance between the halo neutrons. It is of notice that in this case, renormalization effects due to the clothing of single-particle states by vibrations, in particular the lowest lying quadrupole vibration of the core ^9Li , are as strong as mean field effects, as testified by parity inversion and the appearance of a new magic number, namely $N = 6$ (cf. Fig. 2.6.3 (I)). Again in this case $s_{1/2}^2(0)$ and $p_{1/2}^2(0)$ are not correlated in Ω_{12} , while the Cooper state probability density displays a clear angular correlation (see Fig. 2.6.3 (II) (a) and (b)). Nonetheless, the average distance between the partners of the neutron halo Cooper pair, is considerably larger than that associated with the ^9Li core nucleons, as testified by the following figures (cf. also Fig. 3.2.2):

$$\text{a)} \quad R(^{11}\text{Li}) = 4.58 \pm 0.13 \text{ fm} \quad (V = (4\pi/3)R^3 = 402.4 \text{ fm}^3) \quad \text{see } X \quad (3.2.21)$$

$$\text{b)} \quad R_0(^{11}\text{Li}) = 2.7 \text{ fm} \quad (V = 82.4 \text{ fm}^3) \quad (3.2.22)$$

$$\text{c)} \quad R_0(^9\text{Li}) = 2.5 \text{ fm} \quad (V = 65.4 \text{ fm}^3), \quad (3.2.23)$$

and associated mean distance between nucleons,

$$\text{a)} \quad \left(\frac{402.4 \text{ fm}^3}{2} \right)^{1/3} \approx 5.9 \text{ fm}, \quad (3.2.24)$$

$$\text{b)} \quad \left(\frac{82.4 \text{ fm}^3}{11} \right)^{1/3} \approx 1.96 \text{ fm}, \quad (3.2.25)$$

$$\text{c)} \quad \left(\frac{65.4 \text{ fm}^3}{9} \right)^{1/3} \approx 1.94 \text{ fm}. \quad (3.2.26)$$

The above quantities are to be compared with the standard definition, X

$$d = \left(\frac{\frac{4\pi}{3}R^3}{A} \right)^{1/3} = \left(\frac{4\pi}{3} \right)^{1/3} r_0 \approx 1.93 \text{ fm}, \quad (3.2.27)$$

consistent with the standard parametrization $R_0 = r_0 A^{1/3}$ of the nuclear radius written in terms of the Wigner-Seitz-like radius r_0 ($= 1.2 \text{ fm}$) of the sphere associated with each nucleon, derived from systematics of stable nuclei lying along the stability valley.

* Brink D. and Broglia (2005), App. C,)

system probed in a (p,t) reaction
corresponding to

3.2. TRANSFER PROBABILITIES, ENHANCEMENT FACTOR

179

3.2.1 Interplay between mean field and correlation length

In Fig. 3.2.1 one displays a schematic representation of two *gedanken experiments*: (a) (*independent particle motion*) non-interacting nucleons confined in a mean field potential, e.g. a Saxon-Woods potential with standard parametrization (Bohr and Mottelson (1969)); (b) *independent pair motion*, nucleons interacting through an effective pairing interaction, sum of a short (v_p^{bare}) and long range (v_p^{ind}) NN -pairing potential, confined by a mean field whose parameters are freely adjusted so as to profit at best the pair coupling scheme.

In other words, one moves from a situation in which one assumes: (a) $H = T + v \approx T + U$ (ansatz $\langle v - U \rangle \approx 0$) to another in which (b) $H = T + v \approx T + U' + v_p^{eff}$ (ansatz $\langle v - U' - v_p^{eff} \rangle \approx 0$ and $|U'| \lesssim |U|$, $|v_p^{eff}| \ll |U'|$). Switching from the first to the second situation pairs of nucleons moving in time reversal states will tend to recede from each other. Now, to the extent that one is interested in describing real nuclei lying along the stability valley like e.g. ^{120}Sn , one will rightly posit that the ansatz (a) is more realistic than (b), in keeping with the fact that $(U' + v_p^{eff})$ represent a much smaller fraction of v than U does. Consequently, the right view seems to be that of (a) plus pairing, in which case Cooper-pair partners approach each other, if nothing else, because of angular correlation¹⁶. The "correctness" of picture (b) reemerges, as already stated, e.g. in connection with transfer reactions, also in keeping with the fact that one- and two-particle transfer absolute cross sections have the same order of magnitude. And it is likely that picture (b) becomes quite useful in discussing the structure of light halo nuclei.

Within this context we note that the fact that $^9\text{Li}_6$ is well bound ($N = 6$ isotope parity-inverted closed shell), $^{10}\text{Li}_7$ is not while $^{11}\text{Li}_8$ is again bound, indicates that we are confronted with a pairing phenomenon. Allowing the two neutrons moving outside $N = 6$ closed shell to correlate in the configurations $j^2(0)(s_{1/2}^2, p_{1/2}^2, d_{5/2}^2 \dots)$ through a short range bare pairing interaction, e.g. the v_{14} Argonne NN -potential, does not lead to a bound state. The system lowers the relative momentum of the pair exchanging at the same time the low-lying dipole vibration of the associated diffuse system becoming, eventually, bound, ever so weakly ($S_{2n} = 380$ MeV). The radius of the resulting system ($R(^{11}\text{Li}) = 4.58 \pm 0.13$ fm) corresponds, in the parametrization $R_0 = 1.2A^{1/3}$ fm, to an effective mass $A \approx 60$. So undoubtedly the system has swelled in moving from $A = 9$ to $A = 11$ in a manner that goes beyond the $1.2A^{1/3}$ (fm) expected dependence. Although the correlation length of the neutron Cooper is restricted to $2 \times R(^{11}\text{Li}) \approx 9$ fm, half of the estimated value $\xi \approx 20$ fm, it is double as large as $2 \times R_0(^{11}\text{Li}) \approx 5.4$ fm. Consequently, the function $(|\Psi_0(\mathbf{r}_1, \mathbf{r}_2)|^2)$ displayed in Fig. 2.6.3 (II) b) should be read with care. It is also noted that the associated mean field potential can be parametrized in terms of a standard Woods-Saxon potential (see Bohr and Mottelson (1969), Eq. (2-182) p. 239) of depth $U' \approx -36$ MeV, much weaker than the typical value of $U \approx -50$ MeV.

¹⁶Bertsch, G. F. et al. (1967); Ferreira, L. et al. (1984); Matsuo, M. (2013) and refs. therein.

situations

target of
pickup react
induced in
a heavy ion
collision between
superfluid
nuclei, in
which

Within
this context,

a situation which can eventually materialize also in connection with nuclear excited states.

CHAPTER 3. SIMULTANEOUS VERSUS SUCCESSIVE TRANSFER

It will be surprising if this bootstrap-like mechanism to profit from very low, (unstable) nuclear densities to generate transient medium polarization effects which acting between Cooper pair partners (separated by distances of the order of ξ) to eventually stabilize a halo system, was a unique property of ^{11}Li . In fact, one can expect particular situations of s and p states at threshold eventually leading to a symbiotic halo Cooper pair with such a small value of S_{2n} , which eventually gives rise to a value of $2R \approx \xi$. A problem in the quest of such exotic, but standard Cooper pair picture in condensed matter superconductors, may be related in the nuclear case to the very short lifetime of the resulting system (within this context one is reminded of the fact that $\tau_{1/2}(^{11}\text{Li}) = 8.75 \text{ ms}$).

In the above discussion, mention has been made to a bootstrap generation of infinite, condensed-matter-like situation (also in connection with Fig. 3.7.1, in which one was referring to finite density overlap across barriers between superfluid nuclei). Let us remind us that such a methodologic approach is no new to nuclear physics. For this purpose we can use as example the definition of a nuclear temperature and of the associated energy reservoir which can be shared statistically. How does one make a heat reservoir in the nucleus? While it is not a thermal bath in the classical sense, when the system emits a neutron or a γ -ray in the cooling process, it exchanges energy statistically with the freed particle. This is in keeping with the fact that the energy distribution of the emitted nucleon or γ -ray is determined by the density of levels of the daughter states (Bortignon, P. F. et al. (1998)). Concerning the γ -decay of the compound nucleus, it proceeds through $E1$ -transitions, essentially profiting of the Axel-Brink ansatz introduced in nuclear physics to deal with this types of cooling processes. Within the bootstrap ansatz of symbiotic Cooper pair binding, we introduce a straightforward generalization of the Axel-Brink hypothesis based on well established experimental results. Namely the fact that the line shape and thus also the percentage of EWSR per energy interval as well as the decay properties of the GDR will reflect the static (splitting) and dynamic (motional narrowing) deformation properties of the state on which the GDR is built upon.¹⁷

In the case of halo nuclei this generalization is not only quantitative but also qualitative. A sensible fraction of the TRK sum rule is found almost degenerate with the ground state. From the elastic antenna-like response typical of the high energy ($\hbar\omega_{GDR} \approx 80 \text{ MeV}/A^{1/3}$) GDR one is now confronted with a very low energy ($\lesssim 1 \text{ MeV}$) plastic dipole response (GDPR). Regarding the consequences this phenomenon has for the $L = 1$ induced interaction between nucleons, one moves from dipole-dipole (static moment interactions) to dispersive (retarded) contributions, emerging essentially from quantum mechanical ZPF. In other words, and making use of an analogy with atomic physics, one moves from an interaction between polar molecules, to a "purely" quantal interaction arising from the mutual polarization of one molecule in the rapidly changing field of the other (due to

¹⁷ Le Tourneau (1965); Bohr, A. and Mottelson (1975); Bortignon, P. F. et al. (1998) and refs. therein.

is

\lesssim
 $(\lesssim 1 \text{ MeV})$

an s.p. at threshold
based

the instantaneous configuration of electrons and nuclei associated with ZPF) and viceversa, only one operative in the case of non-polar molecules. It is this second one which dominates the van der Waals interaction (App. 2.D) and, similarly, it is one which can lead to an almost resonant gluing of Cooper pair halos, a mechanism found also at the basis of superconductivity in metals. In other words, the extension of the Axel-Brink hypothesis within the present context allegedly implies to move from a possibility to a must. If one sees a halo, one expects a GDR.

The challenges faced to learn about the physical basis of pairing in nuclei are comparable to those encountered to extract a collective vibration from a background much larger than the signal, as it was the case in the discovery of the GDR in hot nuclei.¹⁸ In trying to observe the full range of pairing effects in nuclei, one has the advantage to start with the system at zero temperature for free. On the other hand one needs to subtract the very large, state dependent effects of the "external" mean field, a challenge not second to that faced by condensed matter practitioners to study low-temperature superconductivity in general, and the Josephson effect in particular.

3.3 Correlations between nucleons in Cooper pair tunneling

Let us call x_1 and x_2 the coordinates of the Cooper pair partners. Let us furthermore assume they can only take two values: 0 when they are bound to the target nucleus, 1 when they have tunneled and become part of the outgoing particle (see Fig. 3.3.1).

The correlation between the two nucleons is measured by the value¹⁹

$$\langle x_1 x_2 \rangle - \langle x_1 \rangle \langle x_2 \rangle = \int d\gamma P_2 \times 1 \times 1 - \int d\gamma P_1 \times 1 \int d\gamma' P'_1 \times 1 = P_2 - P_1 P'_1, \quad (3.3.1)$$

$d\gamma$ being the differential volume in phase space, normalized with respect to the corresponding standard deviations, that is, with respect to

$$\sigma_{x_1} \sigma_{x_2} = \left[(\langle x_1^2 \rangle - \langle x_1 \rangle^2) (\langle x_2^2 \rangle - \langle x_2 \rangle^2) \right]^{1/2}. \quad (3.3.2)$$

Making use of the fact that

$$\langle x_1^2 \rangle = \int d\gamma P_1 \times 1^2 = P_1, \quad (3.3.3)$$

and

$$\langle x_1 \rangle = \int d\gamma P_1 \times 1 = P_1, \quad (3.3.4)$$

¹⁸ See e.g. Bortignon, P. F. et al. (1998) Figs. 1.4 and 6.8, and refs. therein.
¹⁹ Basdevant and Dalibard (2005).

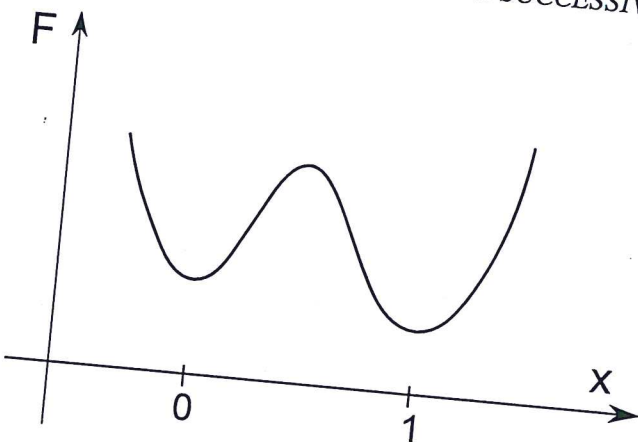


Figure 3.3.1: A schematic representation of nucleon tunneling between target and projectile. The free energy $F = U - TS$ which for the zero temperature situation under consideration (e.g. $^{120}\text{Sn}(p, d)^{119}\text{Sn}$, $^{120}\text{Sn}(p, d)^{118}\text{Sn}$) coincides with the potential energy as a function of the nucleon coordinate x . For $x = 0$ the nucleon is assumed to be bound to the target system. For $x = 1$ the nucleon has undergone tunneling becoming bound to the outgoing particle. In other words x_1 jumps from the value 0 to the value 1 in the tunneling process ($x_1, 0 \rightarrow 1$), the same for the coordinate of the second nucleon.

one
or

(can calculate)
One obtains the function which measures the correlations between nucleons 1 and 2, namely,

$$C = \frac{\langle x_1 x_2 \rangle - \langle x_1 \rangle \langle x_2 \rangle}{\sqrt{(\langle x_1^2 \rangle - \langle x_1 \rangle^2)(\langle x_2^2 \rangle - \langle x_2 \rangle^2)}} = \frac{P_2 - P_1 P'_1}{\sqrt{(P_1 - P_1^2)(P'_1 - P'^2_1)}}. \quad (3.3.5)$$

Because both nucleons are identical and thus interchangeable, $P_1 = P'_1$. Thus

$$C = \frac{P_2 - P_1^2}{P_1 - P_1^2}. \quad (3.3.6)$$

Making use of the empirical values

$$P_1 \approx P_2 \approx 10^{-3} \quad (3.3.7)$$

leads to,

$$C = \frac{10^{-3} - 10^{-6}}{10^{-3} - 10^{-6}} \approx 1. \quad (3.3.8)$$

In other words, within the independent pair motion regime, nucleon partners are solidly anchored to each other: if one nucleon goes over, the other does it also. This is so in spite of the very liable and fragile structure of the nuclear Cooper pairs

l	p_l
0	1.02×10^{-3}
1	2.40×10^{-3}
2	1.26×10^{-2}
3	1.84×10^{-2}
4	6.13×10^{-3}
5	1.39×10^{-3}
6	2.89×10^{-4}
7	5.04×10^{-5}
8	6.51×10^{-6}
9	5.87×10^{-7}

✓ Table 3.3.1: Probabilities p_l (see Eq. (3.2.14) and App. 6.B) associated with the reaction ${}^1\text{H}({}^{11}\text{Li}, {}^{10}\text{Li(gs)}){}^2\text{H}$ calculated with the same bombarding conditions as those associated with ${}^1\text{H}({}^{11}\text{Li}, {}^9\text{Li(gs)}){}^3\text{H}$ (cf. Table 6.B.1). It was assumed that the amplitude with which the single particle orbital $s_{1/2}$ enters in the $|{}^{10}\text{Li}(1/2^+)\rangle$ (gs) is $\sqrt{0.5}$ (cf. Eqs. (6.1.1)–(6.1.3)).

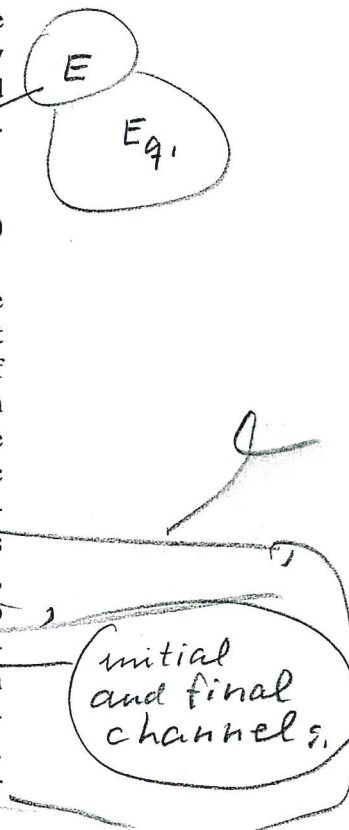
see

($\Delta/\epsilon_F \ll 1$), a clear example of which is being provided by ${}^{11}\text{Li}$. In fact, if one picks-up a neutron from ${}^{11}\text{Li}({}^{11}\text{Li}(p, d){}^{10}\text{Li})$, the other one breaks up essentially instantaneously, ${}^{10}\text{Li}$ being unbound. In spite of this fact, the probability associated with the reaction ${}^{11}\text{Li}({}^{11}\text{Li}, {}^9\text{Li(gs)}){}^1\text{H}$ is (see Table IV Potel et al. (2010) and eq. (2.6.5) as well as Sect. 2.B) given by,

$$P_2 = \frac{5.7 \pm 0.9 \text{ mb}}{2\pi(4.83 \text{ fm})^2} \approx 4 \times 10^{-3}, \quad (3.3.9)$$

a value which is much larger than the value of 4.81×10^{-6} associated with the breakup process mentioned above (see $l = 0$ columns 1 and 3 of Table 6.B.1), let alone $P_1^2 (1.02 \times 10^{-3})^2 \approx 10^{-6}$ as given in Table 3.3.1. One may be surprised of this result, in keeping with the fact that most of the two-nucleon transfer reaction cross section ($\approx 80\%$) is associated with successive transfer (see Fig. 6.B.3). The answer is in any case contained in the relation (3.2.19), applicable both for static and dynamic pair modes, in keeping with the fact that in nuclei, dynamic spontaneous breaking of gauge invariance is of similar importance as the static one.²⁰ It is of notice that in successive transfer processes the one-particle channels are virtual, that is with no outgoing running waves, and thus with a very different coupling to the continuum states than in the case of real asymptotic waves. This coupling influences in an important way the structure aspects of the problem, less the reaction ones. But again, the simple answer is that the halo Cooper pair in its tunneling between ${}^{11}\text{Li}$ and ${}^1\text{H}$ does not see neither ${}^{10}\text{Li}$ nor ${}^2\text{H}$, behaving as an entity. Surprisingly, the regime of independent pair motion extends also to the single pair situation. Two-particle tunneling can specifically probe such a regime.

²⁰ cf. Fig. 2.5.7, cf. also Sect. 3.8 and Fig. 4 Potel, G. et al. (2013b); cf. Fig. 3.3.2



Order parameter $\left(\langle \tilde{0}|PP^\dagger|\tilde{0}\rangle\right)^{1/2} = \begin{cases} \alpha_0 = \sum_{\nu>0} U'_\nu V'_\nu \\ \alpha_{dyn} = \sum_{\nu>0} U_\nu^{eff} V_\nu^{eff} \end{cases}$

pairing vibrations

$$\left(U_\nu^{eff}\right)^2 = 2Y_a^2(j_\nu)/\Omega_\nu; \quad \left(U_\nu^{eff}\right)^2 = 1 - \left(U_\nu^{eff}\right)^2$$

$$\begin{cases} X_n(j_\nu) \\ Y_n(j_\nu) \end{cases} = \frac{\left(\sqrt{\Omega_j}/2\right)\Gamma_n}{2|E_j| \mp W_n}$$

pairing rotations

$$\begin{cases} U'_\nu \\ V'_\nu \end{cases} = \frac{1}{\sqrt{2}} \left(1 \pm \frac{\epsilon_\nu}{\sqrt{\epsilon_\nu^2 + \Delta^2}}\right)^{1/2}$$

✓ Figure 3.3.2: Order parameter associated with static and dynamic pair correlations (see Potel, G. et al. (2013b)).

summing up, a

A direct consequence of the above parlance is the fact that the Cooper pair rigidity emerges from phase coherence (in gauge space), and leads to the generalized rigidity of pairing rotational (static) and vibrational (dynamic) bands which can be instantaneously set into rotation (vibration) with just the push imparted in gauge space by the transferred pair, without this fact violating any limiting velocity, neither of medium propagating signals nor of light.

not italics
but normal
lettering

3.4 Pair transfer

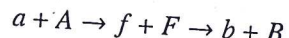
The semiclassical two-nucleon transfer amplitudes fulfill, in the independent particle limit, the relations²¹,

and

$$a_{sim}^{(1)} = a_{NO}^{(1)}, \quad (3.4.1)$$

with

$$a_{succ}^{(2)} = a_{one-part}^{(1)} \times a_{one-part}^{(1)}, \quad (3.4.2)$$



²¹ see App. 5.C, also Potel, G. et al. (2013a).

corresponding to the product of two single nucleon transfer processes. On the other hand, in the **strong correlation limit** one can write, making use of the post-prior representation

$$\tilde{a}_{succ}^{(2)} = a_{succ}^{(2)} - a_{NO}^{(1)}. \quad (3.4.4)$$

Thus

$$\lim_{E_{corr} \rightarrow \infty} \tilde{a}_{succ}^{(2)} = 0, \quad (3.4.5)$$

and all transfer is, in this case, due to simultaneous transfer. Actual nuclei are close to the independent particle limit (E_{corr} (1–2 MeV) $\ll \epsilon_F \approx 37$ MeV). Then successive transfer is the major contribution to pair transfer processes. But successive transfer seems to break the pair *right? Wrong. Why?* let us see below.

3.4.1 Cooper pair dimensions

Typical correlation energies of Cooper pairs are 1–2 MeV. Now, such a system (dineutron or diproton) is not bound and needs of an external field to be confined. This is the role played by the single-particle field (cf. Fig. 3.1.3). Let us now calculate the dimensions of a Cooper pair (correlation length). We start with the relation

$$\delta x \delta p \geq \hbar \quad \delta \epsilon \approx 2E_{corr}, \quad (3.4.6)$$

where

$$\epsilon = \frac{p^2}{2m}; \quad \delta \epsilon = \frac{2p\delta p}{m} \approx v_F \delta p, \quad (3.4.7)$$

and thus

$$\delta \epsilon \approx 2E_{corr} \approx v_F \delta p, \quad (3.4.8)$$

leading to

$$\xi = \delta x = \frac{\hbar}{\delta p} \approx \frac{\hbar v_F}{2E_{corr}} \quad (\text{correlation length}). \quad (3.4.9)$$

Making use of the fact that in nuclei,

$$\frac{v_F}{c} \approx 0.3, \quad (3.4.10)$$

one obtains

$$\xi \approx \frac{200 \text{ MeV fm} \times 0.3}{2 \text{ MeV}} \approx 30 \text{ fm}. \quad (3.4.11)$$

(See Sect. 6, 2, 3) *

Consequently, successive and simultaneous transfer feel equally well the pairing correlations giving rise to long range order. This virtual property can become real in e.g. a pair transfer between two superfluid tin isotopes (Fig. 3.4.1).

Objection

What about $v_{pairing} (= G)$ becoming zero, e.g. between the two nuclei?

²² See von Oertzen, W. (2013)

*) Idini et al (2017)

"From bare to renormalized... " add to list of refs.

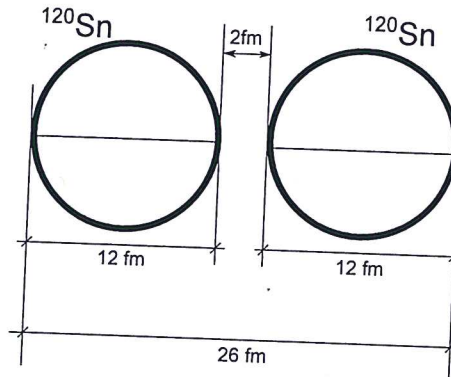


Figure 3.4.1: Schematic representation of two Sn-isotopes (radius $R_0 \approx 6$ fm) at the distance of closest approach in a heavy ion collision.

Answer

$$\frac{d\sigma(a(b+2) + A \rightarrow b + B(A+2))}{d\Omega} \sim |\alpha_0|^2, \quad (3.4.12)$$

$$\alpha_0 = \langle BCS(A+2) | P^\dagger | BCS(A) \rangle = \sum_{\nu>0} U_\nu(A) V_\nu(A+2). \quad (3.4.13)$$

(cf. also App. 3.8.)

Objection

Relation (3.4.13) is only valid for simultaneous transfer, *right? Wrong.*

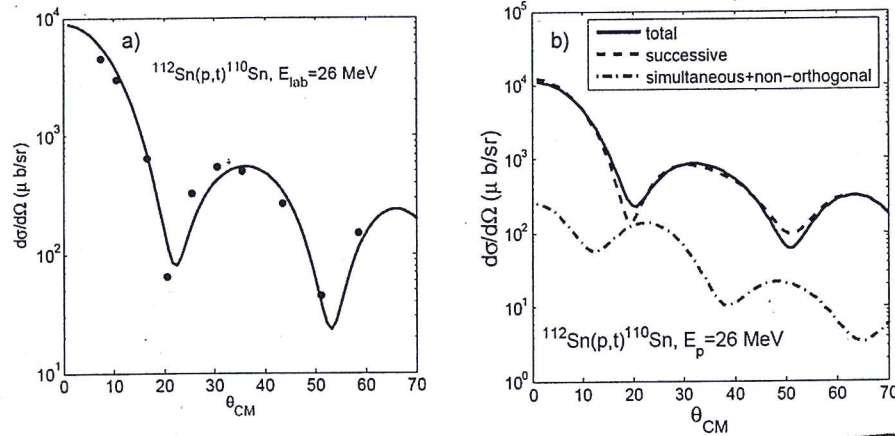
Answer

The order parameter can also be written as,

$$\begin{aligned} \alpha_0 &= \sum_{\nu, \nu' > 0} \langle BCS | a_\nu^\dagger | int(\nu') \rangle \langle int(\nu') | a_\nu^\dagger | BCS \rangle \\ &\approx \sum_{\nu, \nu' > 0} \langle BCS(A+2) | a_\nu^\dagger a_\nu^\dagger | BCS(A+1) \rangle \langle BCS(A+1) | a_\nu a_\nu^\dagger | BCS(A) \rangle \\ &= \sum_{\nu, \nu' > 0} \langle BCS(A+2) | V_\nu(A+2) \alpha_\nu^\dagger \alpha_\nu^\dagger | BCS(A+1) \rangle \\ &\times \langle BCS(A+1) | \alpha_\nu U_\nu(A) \alpha_\nu^\dagger | BCS(A) \rangle = \sum_{\nu>0} V_\nu(A+2) U_\nu(A), \quad (3.4.14) \end{aligned}$$

where the (inverse) quasiparticle transformation relation $a_\nu^\dagger = U_\nu \alpha_\nu^\dagger + V_\nu \alpha_\nu$ was used. Examples of two-nucleon spectroscopic amplitudes involving superfluid targets, namely those associated with the reactions $^{112}\text{Sn}(p, t)^{110}\text{Sn(gs)}$ and $^{124}\text{Sn}(p, t)^{122}\text{Sn(gs)}$ are given in Table 3.4.1. Making use of these amplitudes (first

some of
and 6.2.1.)



✓ Figure 3.4.2: a) Absolute differential cross section associated with the reaction $^{112}\text{Sn}(p,t)^{110}\text{Sn}(\text{gs})$ calculated with the software COOPER (mention in appendix software) in comparison with the experimental data (Guazzoni, P. et al. (2006)). b) Details of the different contributions to the total absolute (p,t) differential cross section (for details see Potel, G. et al. (2013a), Potel, G. et al. (2013b)).

(App. 6,D)

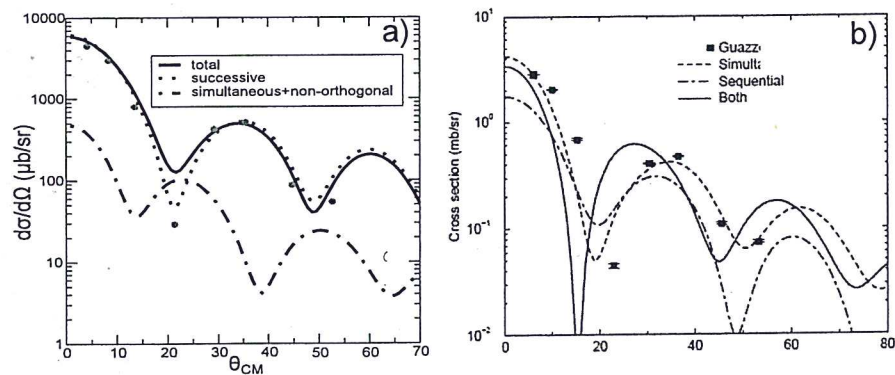


Figure 3.4.3: Absolute differential cross section associated with the reaction $^{124}\text{Sn}(p,t)^{122}\text{Sn}(\text{gs})$ calculated making use of: a) second order DWBA taking into account non-orthogonality corrections and the two-nucleon spectroscopic amplitudes resulting from BCS (see Table 2.4.1, third column; for details see Potel, G. et al. (2013a), Potel, G. et al. (2013b)) in comparison with experimental data (Guazzoni, P. et al. (2011)). b) As above, but making use of FRESCO (reaction) and of shell model two-nucleon overlaps (structure); cf. Table 2.4.1 fourth column (for details cf. Thompson, I.J. (2013)).

(Table 6.2.2)

of Table 2.4.1

App. 6 D →

Gregory, lo
debes comple-
tar respon-
diendo
también
a los
preguntas
de Ben
Mayman.

column) and of global optical parameters, the two-nucleon transfer absolute differential cross section of the reaction $^{112}\text{Sn}(p, t)^{110}\text{Sn}(\text{gs})$ at center of mass bombarding energy of $E_p = 26$ MeV, was calculated making use of the software COOPER based on second order DWBA and taking into account successive and simultaneous transfer properly corrected for non-orthogonality (cf. Chapter 5 and App. 6.D). It is compared with experimental data in Fig. 3.4.2 (a). The corresponding absolute integrated cross sections are $1310 \mu\text{b}$ and $1309 \pm 200 \mu\text{b}$ respectively. The largest contribution to the cross section arises from successive transfer, the cancellation between simultaneous and non-orthogonality amplitudes being important (Fig. 3.4.2 (b)). The above is a typical example of results of a systematic study of two-nucleon transfer reactions in terms of absolute cross sections.²³

Making use of two-nucleon spectroscopic amplitudes worked out within the framework of an extended shell model calculation (Table 2.4.1, second column) one obtains very similar results to those displayed in Fig. 3.4.2 (a). In Fig. 3.4.3 (a) we report results similar to those displayed in Fig. 3.4.2, but for the case of the reaction $^{124}\text{Sn}(p, t)^{122}\text{Sn}(\text{gs})$ calculated within second order DWBA making use of the BCS spectroscopic amplitudes (Table 2.4.1 third column). We display in Fig. 3.4.3 (b) the absolute differential cross section calculated with NuShell spectroscopic amplitudes and the coupled channel software FRESCO.²⁴

Let us now provide an example of two-nucleon transfer around a closed shell nucleus displaying well defined collective pairing vibrational modes. We refer, in particular, to the pair removal mode of ^{206}Pb , that is, to the reaction, $^{206}\text{Pb}(t, p)^{208}\text{Pb}(\text{gs})$. Making use of the spectroscopic amplitudes displayed in Tables 2.5.2 and 2.5.3 and of global optical parameters, the associated absolute differential cross sections was calculated again with the software COOPER. It is displayed in Fig. 3.4.4 in comparison with experimental findings. In the same figure, the total differential cross section is compared with that associated with the TD (Tamm–Dankoff) description of $^{206}\text{Pb}(\text{gs})$, that is, setting the pairing ground state correlations to zero ($\sum_i X_r^2(i) = 1, Y_r(k) \equiv 0$, see Table 2.5.2). In this case, theory underpredicts observation by about a factor of 2, let alone the fact that the TD solution does not conserve the two-nucleon transfer sum rule. Also given in Fig. 3.4.4 is the predicted cross section associated with the pure configuration $|p_{1/2}^{-2}(0)\rangle$. These results underscore the role pairing correlations play in the properties of ^{208}Pb pair removal mode $|r\rangle \equiv |^{206}\text{Pb}(\text{gs})\rangle$. Not only they make the two holes correlate both in angle and, radially on the surface. It lowers the momentum by increasing the volume over which the two fermions are allowed to move (spill-out) and thus correlate, as required by the calculated correlation length ξ .²⁵

It is of notice, that within the effective reaction mechanism described in Sect. 2.1 pairing correlations increase the value of $\Omega_0 (\approx 0.97)$. As a consequence the $l = n = 0$ two-neutron system gives a much larger contribution to the two-nucleon

²³Poté, G. et al. (2013a), Poté, G. et al. (2013b) see also Ch. 6, in particular Fig. 6.2.1.

²⁴Thompson, I.J. (2013).

²⁵Bertsch, G. F. et al. (1967), Ferreira, L. et al. (1984); Matsuo, M. (2013) see also Figs. 2.6.3-a and b) i.e. left part.